



# Long-term leaching mechanisms of Portland cement-stabilized municipal solid waste fly ash in carbonated water

Muberra Andac, Fredrik Paul Glasser \*

*Department of Chemistry, University of Aberdeen, Meston Walk, Old Aberdeen, Scotland AB24 3UE*

Manuscript received 14 January 1998; accepted manuscript 8 June 1998

## Abstract

A leach test is described and applied to municipal incinerator fly ash (10%) stabilized in Portland cement. The test differs from previous tests mainly by bubbling  $\text{CO}_2$  through the leachant, which itself is periodically renewed. An advantage of the test is that pH remains nearly constant at 6.5 to 6.8 throughout the test duration. The results of leach tests are correlated with microstructural studies of the leached layer, which reaches a depth of  $\sim 800 \mu\text{m}$  in 214 days. Development of a complex zonal structure gives a semiprotective surface layer. If the initial slope of the leaching curve as a function of time<sup>1/2</sup> is prolonged, experimental results fall well below this extrapolated curve as leaching times increase beyond  $>100$  to 200 h. Important changes occur in leach mechanisms at about this time, and the predictive accuracy of short-term accelerated tests, particularly when pH is not stabilized, is questioned. © 1999 Elsevier Science Ltd. All rights reserved.

**Keywords:** Microstructure; Long-term performance; Fly ash; Surface layer; Leaching

The incineration of municipal solid wastes (MSW) generates fly ash, disposal of which could present serious environmental and ecological problems because it has a high content of readily released toxic elements [1]. It is desirable to condition the ash before disposal to immobilize the soluble toxic species present. Cement-based systems, especially Portland cement, have been used for this purpose [2]. They provide chemical as well as physical immobilization potential for conditioning of toxic metals. Many leaching methods have been developed to estimate the leach rate and leaching mechanisms of wastes that are placed in landfill [3,4]. The Dutch tank leaching test NEN 7345 was developed in The Netherlands to characterize the leaching behavior of waste materials. This test is claimed to be a rapid and inexpensive way to evaluate the leaching rate of species from cement-stabilized wastes for regulatory purposes [5]. In the test, leaching of components from solid monolithic products is determined by submersing  $4 \times 4 \times 4\text{-cm}$  cubes in initially demineralized water and renewing the leachate at eight fixed times; 2, 8, 24, 48, 72, 96, 168, and 384 h. The concentration of each component in the each leachate is analyzed and the results are presented as a cumulative leached

fraction. In a previous paper [6] it was shown that the test does not, as claimed, elucidate actual leach mechanisms. If this conclusion is correct, it has important implications, because Fick's law of diffusion may not be applicable to extrapolation of short-term test results. The departures were attributed in part to access of atmospheric  $\text{CO}_2$ , which is only partially excluded by a lid, with the result that the pH, initially  $\sim 7$ , increases during the course of the test. During the first few cycles, alkali release from the solid is sufficiently rapid to allow the pH to reach  $\sim 12$ ; however, in subsequent cycles, even though the cycle duration increases, the rise in pH is much less. Bubbling air through the leachant gave a much more stable and constant leach conditions by fixing  $P_{\text{CO}_2}$ .

In the present study, leaching of components from stabilized MSWI fly ash conditioned with ordinary Portland cement (OPC) was analyzed, but the Dutch tank test [5] was further modified. First, because the standard mortar cubes used previously [6] were exhausted, fresh samples had to be cast. These were made as neat paste cylinders containing 10% of MSWI fly ash. Also, the  $\text{CO}_2$  activity was raised by bubbling 100%  $\text{CO}_2$ , at  $\sim 760$  torr, through the leachant to accelerate the test. Moreover, the short-term test procedure (total  $\sim 34$  days) was extended to  $\sim 214$  days. The leaching mechanisms were inferred from leach test results and the microstructure of the leached samples.

\* Corresponding author. Tel.: 44 (0) 1224-272906; Fax: 44 (0) 1224-272908.

Table 1  
Composition of cement and MSWI fly ash

| Wt% oxide component            | OPC   | MSWI fly ash |
|--------------------------------|-------|--------------|
| CaO                            | 62.72 | 20.64        |
| SiO <sub>2</sub>               | 19.17 | 28.34        |
| Al <sub>2</sub> O <sub>3</sub> | 5.06  | 10.42        |
| Fe <sub>2</sub> O <sub>3</sub> | 3.95  | 1.85         |
| MgO                            | 2.18  | 2.60         |
| SO <sub>3</sub>                | 3.28  | 2.90         |
| Na <sub>2</sub> O              | 0.136 | 6.03         |
| K <sub>2</sub> O               | 0.348 | 5.12         |

OPC: ordinary Portland cement; MSWI: municipal solid waste incinerator.

Table 2  
Metal contents of MSWI fly ash

| Element | Wt%  |
|---------|------|
| Zn      | 1.7  |
| Pb      | 0.8  |
| Cd      | 0.03 |
| Cu      | 0.06 |
| Cr      | 0.07 |
| Sn      | 0.16 |
| Mn      | 0.05 |
| LOI*    | 3.48 |

\* Mainly organic char. LOI determined at 550°C.

## 1. Experimental

### 1.1. Materials

The OPC used was made to BS 12, similar to an ASTM type I. The MSW incinerator fly ash, supplied by ECN Petten (Petten, The Netherlands) [5], has a complex structure and consists of a mixture of phases. Chemically it contains mainly Ca, Al, and Si, partly in amorphous form, together with alkali chlorides, soluble sulfates, heavy metal

salts, and an organic phase. The ash properties and characterization data (physical, chemical, and mineralogical) were reported previously [6,7]. Table 1 lists the chemical analysis of main components of OPC and MSWI fly ash. The MSWI fly ash has a relatively high content of toxic metals, mainly Zn and Pb (Table 2).

## 2. Procedure

### 2.1. Preparation of the test specimen

The cement pastes were prepared by mixing cement with MSWI fly ash and double distilled water, respectively, at a water-to-cement + fly ash ratio (w/c) of 0.40; 10% MSWI fly ash (10% of the cement replaced by fly ash) was used in the blend. The mix was cast into cylindrical Perspex molds, aged for 24 h, demolded, and aged at 98–100% humidity at room temperature for 60 days before commencing leaching experiments.

### 2.2. Leaching test

The Dutch tank leaching method was used for cement pastes in normal and modified form, as described earlier. The leaching experiments were performed at room temperature, ~20°C. The specimen tank was filled with double distilled water to achieve L/S = 2.46. CO<sub>2</sub> was bubbled continuously into the vessel as a form of accelerated test. The leachate was removed and replaced after 2, 8, 24, 48, 72, 96, 168, and 384 h and 1, 2, 3 months (giving a total leaching time of ~214 days). The same volume of leachant was used for each renewal.

The leachates were filtered through a 0.45-μm membrane filter to remove particulates and larger colloids and, after measurement of pH, acidified with 1M HNO<sub>3</sub> to pH 2 ± 0.5 and analyzed for selected elements (Na, K, Li, Ca, Mg, Al, Si, Fe, Zn, Cd, Pb, Ba, and Sr). The analyses of elements present in the aqueous phase at low concentrations of Al, Fe, Sr, and Ba were done by inductively coupled plasma-mass spectroscopy (ICP-MS); atomic absorption spectroscopy

Table 3  
pH and % cumulative leach data for PC + 10% MSWI fly ash paste in continuously CO<sub>2</sub> bubbled water at ~20°C

| Leach time (h) | No. of renewals | pH   | Na         | K          | Li         | Ca        | Mg         | Al         |
|----------------|-----------------|------|------------|------------|------------|-----------|------------|------------|
| 2              | 1               | 6.74 | 2.96 (10)  | 3.93 (3)   | 1.17 (1)   | 0.019 (1) | 0.010 (1)  | 0.0012 (1) |
| 8              | 2               | 6.95 | 6.73 (21)  | 8.89 (4)   | 2.85 (4)   | 0.082 (1) | 0.058 (2)  | 0.0021 (1) |
| 24             | 3               | 6.47 | 12.11 (36) | 15.95 (7)  | 5.44 (5)   | 0.106 (1) | 0.233 (3)  | 0.0022 (1) |
| 48             | 4               | 6.77 | 18.19 (55) | 23.97 (9)  | 8.69 (6)   | 0.170 (1) | 0.507 (3)  | 0.0024 (1) |
| 72             | 5               | 6.49 | 22.04 (58) | 28.51 (6)  | 12.13 (9)  | 0.211 (0) | 0.867 (2)  | 0.0025 (1) |
| 96             | 6               | 6.89 | 28.39 (53) | 35.94 (2)  | 15.87 (10) | 0.224 (2) | 1.270 (1)  | 0.0029 (1) |
| 168            | 7               | 6.57 | 35.70 (48) | 43.96 (2)  | 19.99 (2)  | 0.239 (3) | 1.791 (8)  | 0.0032 (2) |
| 384            | 8               | 6.49 | 44.55 (45) | 52.59 (4)  | 25.00 (1)  | 0.251 (4) | 2.426 (4)  | 0.0034 (2) |
| 720            | 9               | 6.68 | 53.87 (40) | 62.17 (8)  | 32.41 (5)  | 0.278 (4) | 2.954 (1)  | 0.0038 (1) |
| 1440           | 10              | 6.84 | 65.12 (36) | 72.31 (10) | 40.93 (7)  | 0.317 (5) | 3.280 (15) | 0.0040 (1) |
| 2160           | 11              | 6.52 | 71.49 (44) | 79.55 (11) | 46.70 (15) | 0.347 (6) | 3.715 (17) | 0.0041 (2) |

(continued)

copy (AAS) was used to analyze for Ca, Mg, and Si. Several tests were made using a spectrophotometer for Al and Si, but the precision and accuracy of the ICP-MS measurements appeared to be comparable to those of the AAS and spectrophotometric methods. As an additional check of the analysis results, each leachate was analyzed three times; the mean values are reported in tables. The percent cumulative leach values were calculated after each renewal.

At the end of leaching, after about 214 days, the solid samples were analyzed by scanning electron microscopy (SEM) and electron microprobe analysis (EMPA). Specimens for microstructural examination were embedded in epoxy resin and polished with successively finer grade diamond pastes down to 0.25  $\mu\text{m}$ . The flat polished samples were coated with carbon, examined by SEM using a JEOL 840 microscope fitted with an energy dispersive X-ray detector and a Cameca electron microprobe analyzer with wavelength dispersive spectrometers.

The bulk chemical composition of the leached sample surface was analyzed. The surface material (up to 200–400  $\mu\text{m}$  thick) could be removed readily from the sample surface using a steel blade. The surface material thus removed was brought into solution with  $\text{LiBO}_2$  fusion [7–9] after particle size reduction to  $<125 \mu\text{m}$ .

### 3. Results

#### 3.1. Leach test results

The leached fractions were analyzed for pH and for selected major and minor matrix components. Major components leached include those that were expected to be weakly bound to the solids that comprise the matrix (Li, Na, K) as well as some that are more strongly bonded (Ca, Mg, Al, Si, and Fe). Five key trace elements were monitored selectively: Zn, Cd, Pb, Sr, and Ba. The mean results, with standard deviations, are given in Table 3. The cumulative fraction leached is relative to the total amount of the relevant species in the sample, MSWI fly ash as well as cement.

These totals were determined after fusion of a weighed sample in  $\text{LiBO}_2$ .

The pH and percent cumulative leach values of the modified test, using continuously bubbled  $\text{CO}_2$ , are plotted against time or square root of time in Figs. 1 and 2, respectively.

The pH of the leachate remained virtually constant during the course of the test, ranging from 6.5 to 6.8. The pH of the leachate is mainly controlled by dissolution of  $\text{CO}_2$  in water and leaching of the more soluble species from the matrix. An alkaline environment normally is established by leaching from the cement matrix, but this tendency is countered rapidly by  $\text{CO}_2$  sorption, with the result that the pH of the leachant does not change significantly. Bubbling gas provides a gentle mixing action, so the solution is homogeneous.

The general trend of most of the leach curves up to  $\sim 100$  h shows that an initial slope is established for a few elements: Na, K, Li, and Ca, which is proportional to  $t^{1/2}$ . However, a number of elements show irregularities, for example, Si, Al, Fe, Mg, Sr, and Ba. Nevertheless, the trends established in the short term give way to a regime of generally lower leach rates after  $\sim 100$  h.

However, the slope of the leach curve in this slower regime is not constant. Thus the dependence of the cumulative fraction leached vs. time must be complex; if the  $t^{1/2}$  “law” is obeyed, the time required to achieve a constant slope must be greater than the duration of the experiments,  $\sim 214$  days. The changes of slope were explained partly by microscopic examination of leached samples.

#### 3.2. Microscopic examination of leached samples

The SEM photographs of the leached surface and EMPA images for selected elements are shown in Figs. 3 and 4, respectively. Both were obtained at the conclusion of the test, after  $\sim 214$  days of leaching. The images disclose some surface erosion and a complex zoned structure in the partially leached matrix.

Backscattered images give a contrast proportional to the mean atomic number and density of the matrix. Because the

Table 3  
Continued

| Leach time<br>(h) | Si        | Fe         | Zn         | Pb         | Cd         | Sr         | Ba         |
|-------------------|-----------|------------|------------|------------|------------|------------|------------|
| 2                 | 0.003 (1) | 0.0010 (1) | 0.0014 (2) | 0.0011 (1) | 0.142 (6)  | 0.082 (3)  | 0.017 (1)  |
| 8                 | 0.012 (1) | 0.0038 (1) | b.d.       | 0.0013 (1) | b.d.       | 0.340 (4)  | 0.085 (1)  |
| 24                | 0.061 (2) | 0.0064 (1) | 0.0018 (2) | b.d.       | b.d.       | 0.815 (5)  | 0.210 (3)  |
| 48                | 0.120 (1) | 0.0158 (1) | b.d.       | b.d.       | b.d.       | 1.525 (6)  | 0.398 (11) |
| 72                | 0.208 (1) | 0.0197 (4) | b.d.       | b.d.       | b.d.       | 2.090 (9)  | 0.530 (19) |
| 96                | 0.297 (1) | 0.0306 (5) | b.d.       | b.d.       | b.d.       | 2.912 (10) | 0.725 (27) |
| 168               | 0.378 (1) | 0.0316 (5) | b.d.       | 0.0021 (1) | b.d.       | 3.200 (12) | 0.774 (29) |
| 384               | 0.435 (2) | 0.0330 (5) | 0.0035 (2) | 0.0023 (1) | b.d.       | 4.134 (17) | 0.939 (20) |
| 720               | 0.492 (2) | 0.0334 (5) | 0.0083 (4) | 0.0034 (1) | 0.417 (25) | 4.622 (21) | 0.989 (22) |
| 1440              | 0.532 (2) | b.d.       | 0.0085 (1) | 0.0038 (2) | b.d.       | 5.225 (27) | 1.111 (24) |
| 2160              | 0.576 (2) | b.d.       | 0.0119 (6) | 0.0040 (2) | 0.946 (36) | 6.181 (30) | 1.352 (33) |

Continuation sections are in the same format.

b.d.: below analytical detection in individual portions.

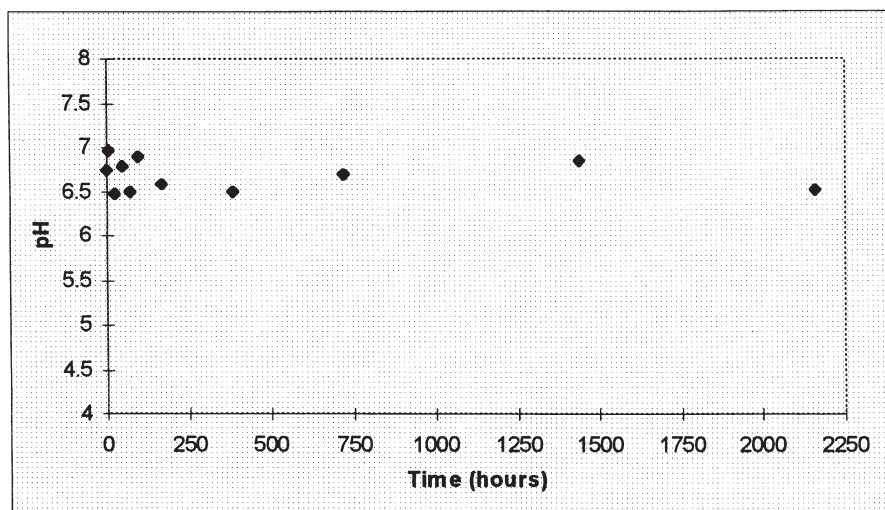


Fig. 1. pH of leachant at the conclusion of a leach cycle. See text for conditions.

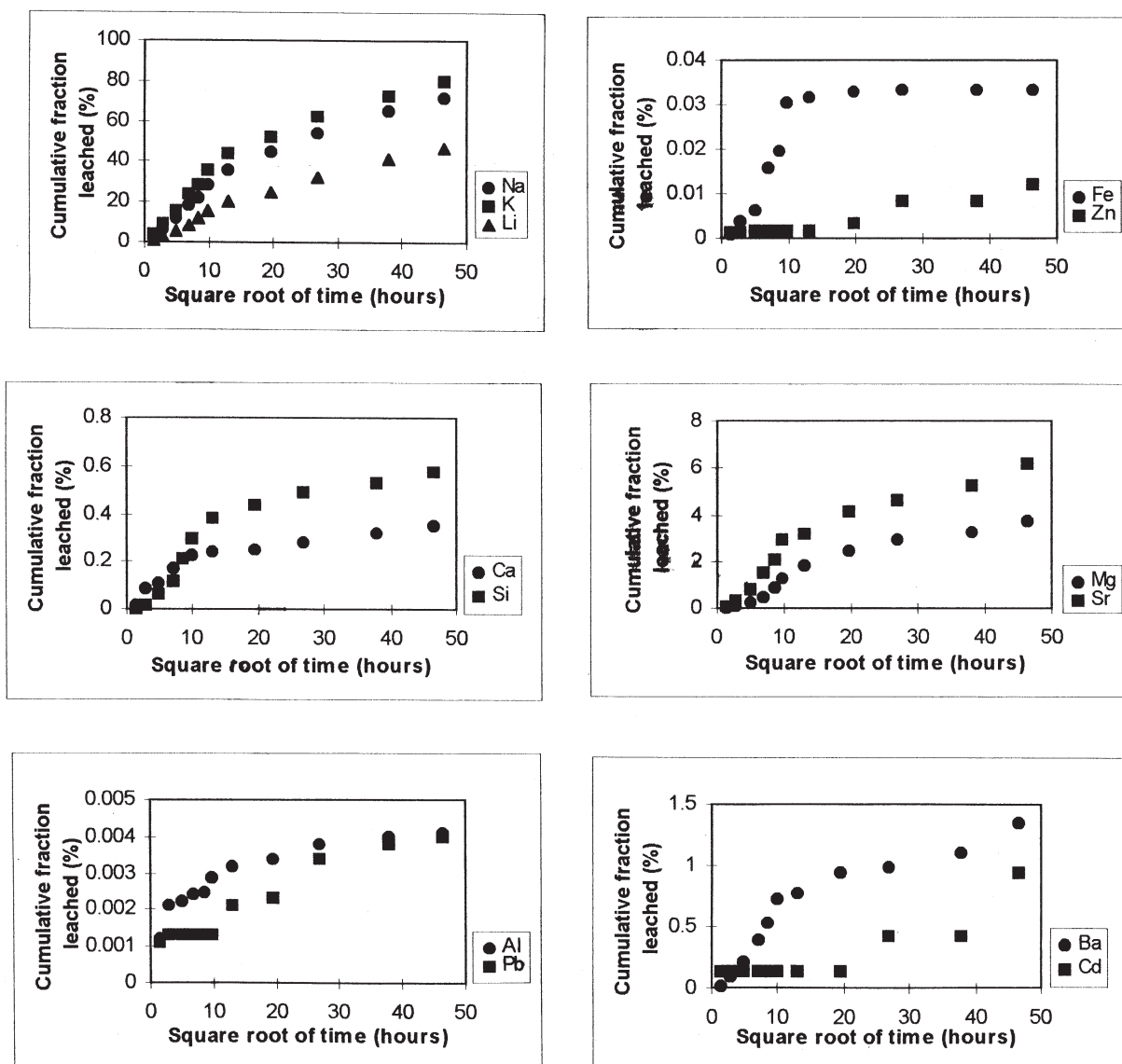


Fig. 2. Cumulative leached fractions of Na, K, Li, Ca, Si Al, and Pb. See text for conditions.

mean atomic numbers of the various cement components do not differ greatly, the images give an indication of local density. Five different zones differing in density, composition, and mineralogy are encountered; their compositions can be established from the combined backscattered electron and chemical images: only those for Ca, Al, Si, S, and K are shown. Color contrast can be used to depict chemical differences on a relative scale, but the representation depicted here is in black and white, which conveys only a limited impression of the visual clarity of the images.

A complex zonal structure develops spontaneously. These zones, designated I to V, are as follows. A very thin zone (I) occurs near the surface. It is low in Ca and extends to a depth of 200 to 300  $\mu\text{m}$ , beneath which occurs a cracked zone (II), followed by another leached zone (III), also low in Ca, and extending 100 to 200  $\mu\text{m}$  deeper. This is underlain by a more calcium-rich zone (IV)  $\sim 80$   $\mu\text{m}$  thick and finally by a lightly leached zone (V), which blends gradually into unaltered matrix. The total cumulative thickness of zones I to V has attained 600 to 800  $\mu\text{m}$  in 214 days, although the cumulative leach values (Fig. 2A) show that Na and K leaching must extend to much greater depths to account for the high cumulative leached fraction of these two elements. The zoned structure of the first  $\sim 1$  mm is

well delineated by several minor elements—sulfur, chloride, and magnesium—and the physical cracking in zone II remains a constant marker to assist comparison between various chemical images. Sulfur, chloride, and magnesium are, in part, concentrated into the unaltered matrix. Potassium and sodium are overall leached, but significant concentrations are retained in the outer leached layers, perhaps surprisingly so given the overall high depletion of alkali. The highly leached zones, I and II, consist mainly of Al, Si, and Ca, together with minor contents of the other elements. Their averaged elemental compositions are given in Table 4.

Zone IV was analyzed with transmission electron microscopic energy dispersive X-ray analysis to obtain microdiffraction evidence of the identify of the phases in this calcium-rich zone. The electron diffraction patterns disclose that two polymorphs of  $\text{CaCO}_3$ , vaterite and calcite, are present.  $\text{CaCO}_3$  can occur in cement as three polymorphs: aragonite, calcite, and vaterite. Their densities are 2.94 to 2.95, 2.71 to 2.94, and 2.64  $\text{g}/\text{cm}^3$ , respectively. Vaterite thus has the lowest density, followed by calcite and aragonite. Assuming a constant flux of Ca and  $\text{CO}_2$  to the zone of carbonate precipitation, the ability to block pores decreases with increasing density, so the presence of low-density vaterite is regarded as contributing most to a decrease of porosity in this zone. The silica content was not matched by a diffraction pattern, and silica is presumed to be present as an amorphous, gel-like material that also contributes to space filling.

Zone IV was analyzed by EMPA and contrasted with the comparatively unleached core; results are given in Table 5. Zone IV concentrates some heavy metals, notably Pb and Ni. However, is unlikely that sufficient accumulation of heavy metals occurs in this zone to alter significantly the mass balances, given the low total volume of this zone relative to the whole sample, but it does appear to impede diffusion of these metals.

The EMPA images also show that cracking must be an additional factor that affects leaching. There are two principal directions of cracks: those normal to the surface and those parallel to the surface. The cracks normal to the surface are characteristically narrow,  $<1$   $\mu\text{m}$ , and in some aspects appear to be partly rehealed by precipitation. The cracks parallel to the leached surface are typically wider,  $\sim 1$  to 2  $\mu\text{m}$ , in electron micrographs but their apparent width may be somewhat enhanced by specimen preparation. This principal crack network tends to separate highly leached zones from comparatively unleached zones. Although the leached zone is, overall, semiprotective, spalling could open up relatively fresh surface to attack if the leached layer becomes mechanically detached. This process is not considered too important at plane surfaces if the cement is mechanically constrained. Nevertheless, cracks are physically very important, because cracking of the solid matrix can significantly increase the apparent bulk permeability, facilitating entry of leachant, which will, in turn, enhance leaching: diffusion of components through a crack is typically faster than through the solid matrix.



Fig. 3. Backscattered electron image of a cut cross-section of the leached surface (top) after 210 days.

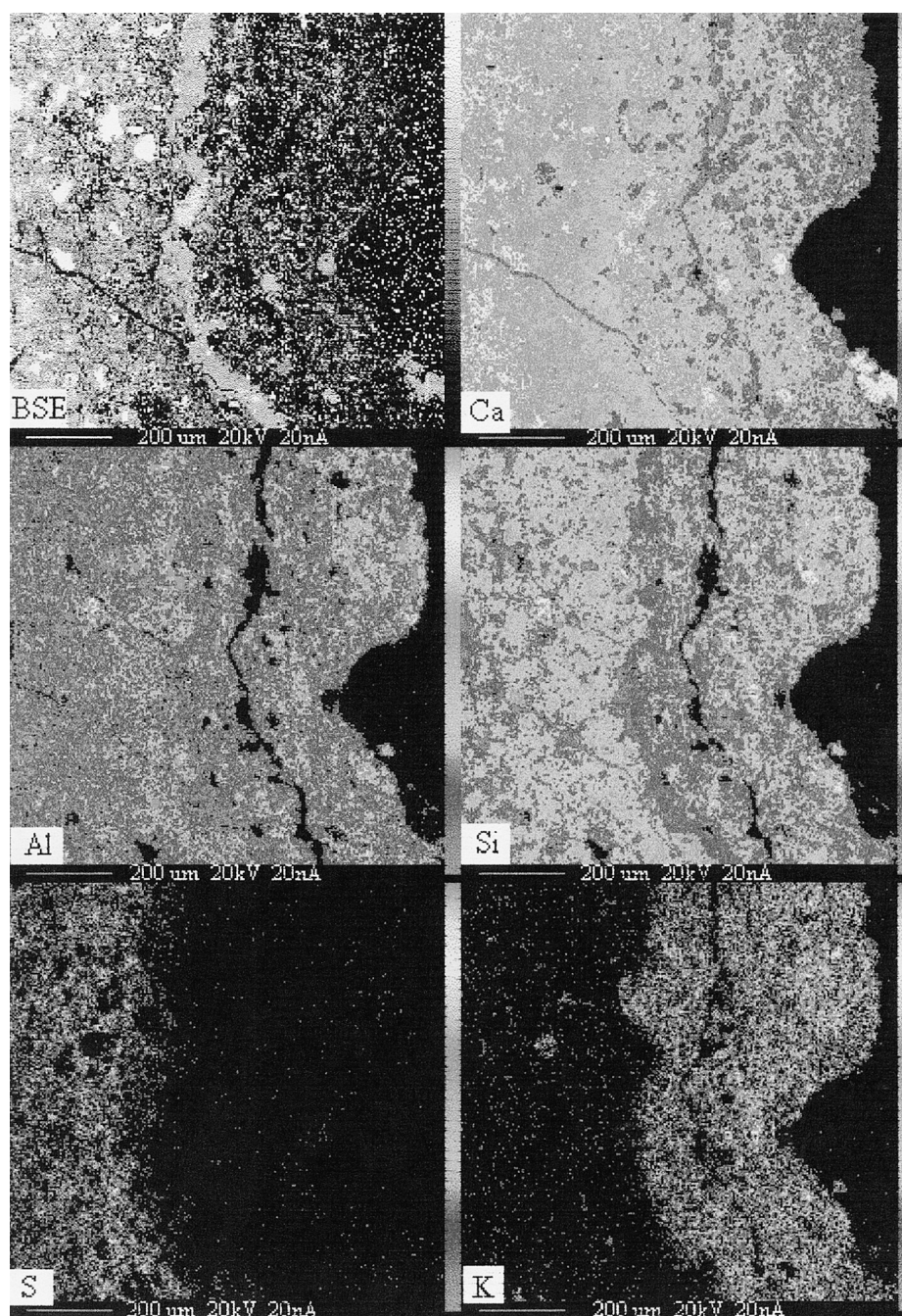


Fig. 4. Backscattered and element-selective images of leached OPC + 10% MSWI fly ash–cement Blend. The blend was cured at  $\sim 20^{\circ}\text{C}$  and 100% relative humidity for 60 days before commencing the leach test. The leachant was  $\text{CO}_2$ -saturated water, renewed according to the schedule given in the text. Total leach duration was 210 days. The outermost leach surface is oriented toward the right-hand side of the images. A key along the right-hand side shows the gray scale assigned to concentration from lowest (bottom) to highest (top).

#### 4. Discussion

$\text{CO}_2$  bubbled tests are arguably more representative of the actual leaching environment of cement-conditioned ash than the standard test using distilled water. In shallow burial in temperate climate soils, potential leachant solutions react strongly with biogenic and atmospheric  $\text{CO}_2$ , which raises  $P_{\text{CO}_2}$  and affects leaching mechanisms. We chose to simu-

late nature and accelerate the test by saturating the reviewed leachant with  $\text{CO}_2$ . An advantage of this protocol is that buffering with  $\text{CO}_2$  causes the leachant pH to remain nearly constant and slightly acidic (see Fig. 1). Only one significant pH gradient remains, lying entirely within the cement monolith.

One of the problems with the rapid tank leaching test, as specified in NEN 7345, is that carbon dioxide is neither rig-

Table 4  
Percent elemental composition of leached surface

| Elements | Percent composition of sample (before leaching) | Percent composition of leached surface (200–400 $\mu\text{m}$ ) |
|----------|---|---|
| Na       | 0.34  | 0.27  |
| K        | 0.51  | 0.73  |
| Ca       | 34.5  | 20.3  |
| Mg       | 1.32  | 0.72  |
| Al       | 2.64  | 4.02  |
| Si       | 9.5   | 8.2   |

idly excluded nor is it specifically included as a parameter. In the first few minutes of the rapid leaching test, as originally specified, the pH of the leachant—initially near neutral—increases rapidly to  $\sim 12$ . As it increases, the rate at which leachant absorbs  $\text{CO}_2$  from the atmosphere also increases. The rates of these competitive processes, one tending to raise pH and the other to depress pH, depend rather crucially on test geometry and include some factors that are not defined in the protocol, such as the surface area of leachant solution exposed to the atmosphere and the air tightness of the cover system (if any).

Upon renewal of leachant in the standard protocol, the pH drops abruptly and again rises. This cycle is repeated at each successive renewal. Thus, pH conditions are highly variable throughout the test duration. Because the cumulative rapid test duration is relatively brief, about 34 days, the cemented cubes are only lightly carbonated at the conclusion of the test. Moreover the extent of carbonation varies from face to face. Nevertheless, the formation of partially carbonated surface layers, in conjunction with fluctuating pH of the leachant, make it difficult to evaluate the applicability of the test to realistic disposal situations and to deduce leach mechanisms.

During leaching, a series of complex reactions occur resulting in a sharply zoned, partially leached layer. Thus, an important assumption underlying Fick's law of diffusion through a homogeneous matrix is increasingly inapplicable as the leach profile matures. The presence of composition zones, marked by selective precipitation as well as dissolution, greatly complicates mechanistic interpretations of test data. The main concern is with leached species and, in terms of mass balance, losses are greater than gain. Thus, the matrix tends, on average, to become more porous. The exact relationships between porosity and permeability are not well established, but the enhancement of porosity in some of the outer zones, enhanced by cracking, is so great as almost certainly to contribute to enhanced permeability. On the other hand, the uptake of carbonate gives rise to  $\text{CaCO}_3$  deposition with formation of a densified layer. The deposition is in part diffuse, throughout zones I and II, as well as more concentrated, in zone IV. The pH of the permeating aqueous phase changes with depth. The pH within the matrix, initially  $\geq 13$ , decreases as Na and K, effectively

Table 5  
Quantitative analyses of sample (weight %)

| Ca   | Pb    | Ni    | Zn    | Na    | Si    | Al   |
|--|-------|-------|-------|-------|-------|------|
| Carbonated zone (zone IV): means of eight spot analyses              |       |       |       |       |       |      |
| 30.71  | 0.064 | 0.011 | 0.152 | 0.045 | 4.92  | 1.37 |
| 32.32  | 0.053 | 0.000 | 0.076 | 0.052 | 4.93  | 1.60 |
| 31.52  | 0.053 | 0.018 | 0.171 | 0.037 | 5.16  | 1.31 |
| 30.37  | 0.025 | 0.000 | 0.162 | 0.039 | 6.64  | 1.75 |
| 31.80  | 0.044 | 0.012 | 0.171 | 0.036 | 5.61  | 1.37 |
| 32.97  | 0.048 | 0.000 | 0.093 | 0.046 | 5.11  | 1.29 |
| 37.09  | 0.037 | 0.000 | 0.102 | 0.036 | 1.68  | 0.44 |
| 31.77  | 0.046 | 0.000 | 0.101 | 0.061 | 5.35  | 1.54 |
| Core of sample (unaffected by leaching): means of five spot analyses |       |       |       |       |       |      |
| 31.29  | 0.000 | 0.006 | 0.174 | 0.010 | 9.77  | 1.83 |
| 50.40  | 0.000 | 0.009 | 0.031 | 0.018 | 11.47 | 0.58 |
| 32.36  | 0.000 | 0.003 | 0.182 | 0.010 | 11.52 | 1.02 |
| 31.43  | 0.007 | 0.020 | 0.162 | 0.054 | 5.89  | 1.61 |
| 36.19  | 0.009 | 0.015 | 0.168 | 0.228 | 19.19 | 3.76 |

present as NaOH and KOH in pore fluid, are leached. But as long as  $\text{Ca(OH)}_2$  and C-S-H remain, the pH of the lightly leached and unaffected portions of the matrix cannot decrease throughout much of the leaching process below  $\sim 12$ , thus implying fairly fixed pH gradients between matrix and leachant throughout much of the leaching process.

Carbonate precipitation is believed to occur preferentially in zones where  $\text{CaCO}_3$  solubility is at a minimum, at pH  $\sim 9$ . Thus, zone IV provides a marker, showing where pH is  $\sim 9$ . The zone of active carbonate precipitation changes as a function of  $\text{CO}_2$  activity in the leachant. When  $\text{CO}_2$  access is limited, carbonate precipitation occurs at or near the cement-leachant interface or possibly in the leachant itself. However, as  $\text{CO}_2$  activity increases, precipitation occurs initially at or near the cement surface moving to progressively greater depths within the matrix. The zone of active precipitation of  $\text{CaCO}_3$  appears to be closely associated with cracking, so the contribution of physical deterioration to overall leaching is enhanced by increasing  $\text{CO}_2$  activity.

Other elements also may exhibit complex response to leaching. For example, chloride appears to concentrate at the boundary between nearly unleached and lightly leached zones, suggesting that outward-diffusing chloride is partially trapped, perhaps as Friedel's salt. Comparing the two sets of test conditions, in the NEN 7345 test, pH fluctuates from  $\sim 7$  to  $\sim 12$  during each renewal, whereas bubbled air and  $\text{CO}_2$  buffer a constant pH. The aqueous  $\text{CO}_2$  activity fluctuates greatly, but in an uncontrolled manner, in the NEN 7345 test, but it remains constant in the bubbled air and  $\text{CO}_2$  tests: as  $P_{\text{CO}_2}$  increases, the equilibrium pH also decreases.

In the three sets of test conditions, the effective  $\text{CO}_2$  activity increases from a low but unknown value in the NEN 7345 test, to 4 torr (air-bubbled) as used in [6] and to 760 torr ( $\text{CO}_2$  bubbled). The impact on leachability is controlled by three factors: increasing mean acidity of the leachant, development of a complex zoned structure in the solid, and

differing extents of cracking. The lower pH of the CO<sub>2</sub>-bubbled test provides a marked degree of acceleration. However, the severity of cracking increases as P<sub>CO<sub>2</sub></sub> increases and, as a consequence, the zone of CaCO<sub>3</sub> precipitation moves deeper into the solid. In comparing results, note that the CO<sub>2</sub>-bubbled test was made with neat cement rather than as in other sets of test data, e.g., in [6] with mortars. The severity of cracking may be affected, as mortars tend to restrain dimensional changes rather better than pastes.

Leachability is thus a complex function of the aqueous chemistry of the leachant, changes to the substrate (permeability, cracking, mineralogical, chemical, etc.), and of the particular chemistry of the leached species. If relative leachability trends are compared, changes in CO<sub>2</sub> activity do not much affect the leachability of Na, K and Ca. However, divalent ions, notably Mg, Sr, Ba, and Cd, are more strongly leached in the slightly acidic environment achieved in the bubbled CO<sub>2</sub> test.

The development of complex chemical and mineralogical gradients suggest that straightforward application of Fick's laws of diffusion is unlikely, except fortuitously, to enable the leach behavior to be modeled: note the departures from ideality in the square root of time plots. Indeed, the suggestion might be made that, although Fickian diffusion is more or less applicable to describe the initial leach behavior, at which point the matrix is relatively homogeneous, it becomes progressively less applicable as leaching progresses, especially for those components whose behavior is influenced by the ensuing mineralogical and chemical zonation. Cracking is an additional complication that affects the leaching of all components. Thus, we are far from having a rapid test that predicts long-term performance with confidence, although the contention that CO<sub>2</sub> activity must be controlled, and as a consequence if it is controlled in the range from 4 to 760 torr, iso-pH conditions are spontaneously achieved, marks a step forward to achieving reproducible and realistic conditions. Moreover, because CO<sub>2</sub> is a "natural" constituent of groundwaters the test conforms to what may occur in burial.

## 5. Conclusions

1. The leaching rate of elements depends on testing time and the particular element.

2. In CO<sub>2</sub>-saturated water, the formation of a leached zone, cracking, and crack development within the matrix of a highly carbonated layer markedly affect the leaching rate of components. Increasing departures from Fickian behavior occurs as leaching progresses.
3. The CO<sub>2</sub> test is recommended as a useful replacement for existing leach test methods.
4. Because CO<sub>2</sub> is a normal constituent of groundwaters, especially in shallow burial in temperate climate regimes, it is realistic to assess its impact.
5. Rapid tests are not reliable predictors of long-term behavior.

## Acknowledgments

M. Andac thanks Prof. F.P. Glasser for financial support. The authors thank Alison Coats and Eric Lachowski for technical assistance and acknowledge the Engineering and Physical Science Research Council for a grant used to acquire the EMPA facility.

## References

- [1] The International Ash Working Group, An International Perspective on Characterisation and Management of Residues from Municipal Solid Waste Incineration, Summary Report, December 1994.
- [2] R. Conner, Chemical Fixation and Solidification of Hazardous Wastes, Van Nostrand Reinhold, New York, 1990.
- [3] P.L. Cote, T.W. Constable, Evaluation of experimental conditions in batch leaching procedures, *Resources and Conservation* 9 (1982) 59–73.
- [4] C.L. Perket, W.C. Webster, Literature review of batch laboratory leaching and extraction procedures, in: *Hazardous Solid Waste Testing: First Conference*, ASTM, STP 760, 1981, pp. 7–28.
- [5] H.A. Van Der Sloot, D. Hoede, G.J. De Groot, G.J.L. Van Der Wegen, P. Quevauviller, Intercomparison of Leaching Tests for Stabilised Waste, Petten, The Netherlands, Document ECN-C-94-062, November 1994.
- [6] M. Andac, F.P. Glasser, The effect of the test conditions on the leaching of stabilised mswi-fly ash in Portland cement. *Waste Management* 18 (1998) 309–319.
- [7] M. Andac, Leaching of Cement Stabilised Solid Waste, Ph.D. Thesis, University of Aberdeen, Aberdeen, Scotland, 1997.
- [8] C.O. Ingamells, N.H. Suhr, F.C. Tan, D.H. Anderson, Barium and strontium in silicates, *Analyst* 53 (1971) 345–360.
- [9] J.C. Van Loan, C.M. Parisi, Scheme of silicate analysis based on lithium metaborate fusion followed by atomic absorption spectrophotometry, *Analyst* 94 (1969) 1057–1062.